

Nonreactive wetting kinetics of binary alloys: A molecular dynamics study

M. Benhassine^a, E. Saiz^b, A.P. Tomsia^c, J. De Coninck^{d,*}

^a Department of Materials Science & Engineering, University of Wisconsin – Madison, Madison, WI 53706, USA

^b Centre for Advanced Structural Ceramics, Department of Materials Science, Imperial College of London, London, UK

^c Materials Sciences Division, Lawrence Berkeley National Laboratory, Berkeley, CA 94720, USA

^d Interface and Surface Physics Laboratory, University of Mons, 7000 Mons, Belgium

Received 15 July 2010; received in revised form 12 October 2010; accepted 16 October 2010

Available online 17 November 2010

Abstract

The dynamic wetting of Cu–Ag binary alloys of different concentrations on rigid Ni surfaces is considered via molecular dynamics. The statics of wetting are studied with regard to the alloy concentration. The dynamic data (speed v , dynamic contact angle θ) are compared to the Molecular-Kinetic model by a fitting procedure. To validate the fittings, the microscopic features of the mechanism are studied. The main parameter of this model (the equilibrium jump frequency K_0) is calculated independently in the simulation. The two values, fitted and measured, are compatible, which extends the validity of the MKT theory for alloys. We also observe in our simulations Marangoni effects and Ag demixing in the formation of an adsorbed layer. Our results also seem to indicate that there is an optimum Cu–Ag binary alloy concentration for increasing the speed of wetting.

© 2010 Acta Materialia Inc. Published by Elsevier Ltd. All rights reserved.

Keywords: High-temperature spreading; Alloys; Wetting; Liquid metals; Molecular dynamics

1. Introduction

The study of dynamic wetting at high temperature is a relatively new field because the often aggressive experimental conditions (atmosphere control, equilibration, reaction, etc.) make it difficult to analyze spreading with high resolution and control [1]. Under these reactive conditions, the atomic mechanisms are not fully understood and the models usually developed for high temperature are empirical continuum models that make approximations at the contact line region [2–4].

Models of dynamic wetting that take into account the microscopic features of the interfaces exist but are associated with nonreactive surfaces; therefore drawing comparisons with a reactive system is not straightforward. Developing a fully predictive theory able to describe, up

to an atomic resolution, the dynamic wetting of liquids at high temperature is a challenge. On an experimental level, progress has been made with the use of drop-transfer, dosing setups and high-speed imaging that allow the observation, with good resolution, of the first instants of the spontaneous spreading process under nonreactive conditions, which occurs in less than 20 ms for noble metals on Mo surfaces [1,5–8].

On a par with these novel experiments, molecular dynamics (MD) computer simulations are a very powerful tool for describing atomic mechanisms since the atomic trajectories are resolved in real time. MD simulations of nonreactive wetting of Ag, Cu and Au on nonreactive substrates in a sessile drop configuration [9,10] have been performed by the authors and indicate that the Molecular-Kinetic model of Blake [11,12] is a good candidate for predicting the dynamic spreading data obtained from experiments [5,13] of metals on Mo. In Ref. [6], it was observed in the simulation that Cu and Ag behaved

* Corresponding author.

E-mail address: joel.deconinck@umons.ac.be (J. De Coninck).

differently on fixed Ni lattices, with Ag liquids more prone to form an advancing monolayer ahead of the contact line with a partially wetted drop.

In this study, the Molecular-Kinetic Theory (MKT) is validated by simulations of Ag–Cu alloys of different compositions on Ni and the predictive power of this model is used to detail the effect of concentration on different parameters, such as the triple-line friction (or controlling atomic jump frequency). Alloys are widely used in the industry because they often have a low cost/effectiveness ratio, the properties can be optimized and, in the case of brazing or soldering, they may exhibit low liquidus temperatures. The melting temperature of the eutectic Ag–Cu system is lower than the temperatures of the separate constituents, making it attractive for brazing and soldering; it is also the base of the very popular Ag–Cu–Ti alloy used for brazing ceramics.

Simulations of Ag–Cu binary liquids have been performed by Webb et al. [14] with MD (where the wetting kinetics of the alloys was studied in reactive and nonreactive cases on top of Cu substrates). Usually, alloys are studied under situations where liquid/solid mixing is allowed and dissolution kinetics dictates the speed of the wetting front [15–18]. Here, the spreading Ag–Cu drops is considered with fixed Ni substrates, to mimic a nonreactive system. A study of nonreactive wetting of alloys may be a step back from previously published material but it permits direct comparison of the dynamic contact angle relaxation vs. well validated predictive models such as the MKT model. Dissolution is avoided and the effect of the composition of a binary liquid on the speed of the wetting front and contact angle relaxation is examined with MD. Practically, it has been shown in experiments that even in soluble systems there are situations in which spreading can be so fast that the initial stages are nonreactive, i.e. the liquid front still advances on a flat-unreacted substrate [1,8,19].

2. The model

2.1. The MKT

The MKT of wetting [11,12] describes the dynamic wetting process via the introduction of equilibrium parameters. In this description, spreading is analyzed using reaction rate theory as a complex atomic process with some critical controlling atomic frequency. The parameters of the model are the equilibrium contact angle θ_0 and the controlling frequencies K_0 of jumps of the liquid atoms, the amplitude of which is λ .

It permits the speed v of the triple junction to be related to the dynamic contact angle as follows:

$$v = 2K_0\lambda \sinh\left(\frac{\gamma_{lv}}{2nk_B T}(\cos\theta_0 - \cos\theta_D)\right) \quad (1)$$

where n is the density of adsorption sites on the surface, k_B is Boltzmann's constant and θ_D represents the dynamic contact angle.

Eq. (1) can then be linearized [20] as Eq. (2) if the argument of the $\sinh(\cdot)$ function becomes small and the unknown parameters K_0 , λ and n can be coupled into a single parameter named the triple-line friction ζ_0 , defined as $\zeta_0 = \frac{nk_B T}{K_0\lambda}$ so that:

$$v = \frac{\gamma_{lv}}{\zeta_0}(\cos\theta_0 - \cos\theta_D) \quad (2)$$

This derivation is more convenient in the sense that it leads to a single unknown parameter but the fitting cannot be applied to very high speeds where the general MKT is more prevalent (Eq. (1)). The surface tension is usually assumed to be a constant of the liquid, which is not the case with varying atomic content. Thus fittings were made by coupling the surface tension γ_{lv} (further replaced by the notation γ) with the friction as a single parameter.

2.2. The system studied and the simulation parameters

We use the code LAMMPS from Sandia National Labs [21,22]. The simulations consist initially of randomly distributed Cu–Ag face-centered cubic (fcc) crystals with Cu contents of 0.25, 0.5 and 0.75. The Cu–Ag alloy is composed of 32,000 atoms modeled with the embedded-atom method (EAM) many-body potentials [23,24]. The crystal is equilibrated and melted for 50 ps at 1400 K and then shifted upon a fixed Ni lattice of 3.52 Å before spreading. The substrate is purposely fixed to mimic a nonreactive system. This methodology has been used by the authors in other simulations of pure Ag, Au and Cu on the same substrate [9,10].

The authors have demonstrated in previous simulations that the sessile drop simulations do not permit to yield strict equilibrium conditions in terms of flow [9]. Thus, to measure the different parameters, an equilibrium system comprising a liquid column of 9000 alloy atoms with periodic boundary conditions on top of a fixed Ni substrate of 4093 atoms is employed (called liquid reservoir simulations).

The timestep is 1 fs and configurations were saved every 0.01 ns or 0.001 ns. The atomic velocities were rescaled to account for a temperature of 1400 K in the liquid every 10 fs. Because the substrate was fixed, i.e. the forces calculated on the solid atoms were zero, the temperature rescaling only accounted for atoms in the Cu–Ag drop.

3. Results

3.1. Equilibrium contact angles and base radius

To measure the spreading data, we evaluate the contact angle and base radius of the drops by exploiting the spherical geometry and fitting the drop to a circular-type shape [20,25–27]. To perform this, we divide the simulation domain into boxes of fixed size and the density is calculated. Whenever the density inside a box exceeds a threshold value for the liquid atoms, we have a point corresponding to the

liquid/vacuum interface. These points are then fitted to a circular profile.

For the different concentrations considered, the data are presented in Fig. 1.

Fig. 1 evidences the fact that the dynamic growth of the base radius is non-monotonous with respect to the atomic content in volume, in other words an optimum can be potentially investigated in the wetting speed.

3.2. Dynamics of wetting

To obtain the contact line speed from the $R(t)$ curve, we use as usual [5,9,10] a set of ratios of polynomials fittings (in the form $R = \frac{p_0 + p_1 t + p_2 t^2 + \dots + p_n t^n}{1 + p'_1 t + p'_2 t^2 + \dots + p'_n t^n}$) to determine the speed (by direct derivation), the error bars being determined by the bootstrap method [28] with an error of a few percent on each individual measurement. The polynomial order is varied and the best fit is used (in the case of the presented simulations an order $n = 3$ was successful, in particular, at avoiding negative speeds). The best fit is determined by the consecutive use of a downhill simplex method starting with a randomly distributed initial parameter and a Levenberg–Marquardt algorithm with the fitted simplex parameters as starting points. More details of this method are given in Seveno et al. [29]. The error bars are also determined by the bootstrap method.

In the case of the presented fits, once the speed is generated with the ratio of polynomials, the dynamic data are fitted to a linear MKT model. The linear model, provided the dynamics are fitted toward equilibration, provides less arbitrary parameters, since the jump frequency K_0 becomes coupled with the characteristic jump distance λ into the friction parameter. Furthermore, to allow for varying surface tension, the coupled parameter γ/ζ_0 is used as well as θ_0 . Indeed, the linear fitting has a physical sense when the regime is close to equilibrium, where the arguments of the sinh function become small (the range of data was

linear when the contact angles were lower than 60–50°, removing only 20% of the points at the most). Table 1 summarizes the parameters of the fittings and the dynamics are displayed in Fig. 2. At around even atomic content, the dynamics presents a sharper slope, resulting in a higher γ/ζ_0 (see Fig. 3).

Plotting the fitted equilibrium contact angle vs. bulk alloy content (Fig. 4) reveals that, except for pure Ag, the angle equilibrates at ~ 10 – 30° . It should be noted that these contact angles are comparable to the angle formed by simulations of pure Ag on Cu, as shown by Webb et al. [14] ($\sim 10^\circ$), and typical experiments of Ag ($13 \pm 3^\circ$) and Cu ($23 \pm 3^\circ$) on nonreactive surfaces at 1150 °C [5], the wedge-shaped region being mostly Ag in content. This is not surprising as we expect that demixing in the drop (see below) creates a pure Ag on a fixed Cu layer on top of a fixed Ni solid, which is distinct from a Cu–Ag alloy on a fixed Ni surface.

By a fitting procedure, we show that the linear MKT interpolates the dynamic data quite well. It does not necessarily imply that these parameters have physical meaning. The triple-line friction, being the result of a collective atomic movement, is only accessible in experiments via a fitting procedure. The molecular dynamics tool enables the fits to be validate using a direct calculation of the atomic frequencies parameters. Thus, we apply the methods which were used to measure the jump frequencies K_0 on pure nonreactive liquids to the Cu–Ag alloys [9,10].

3.3. Direct calculation of K_0

With the molecular dynamics tool, it is relatively easy to measure directly the jump frequency appearing in the MKT (related to the friction by the equation $K_0 = \frac{k_B T}{\zeta_0 \lambda^2}$). From the atomic trajectories, the atoms are followed after equilibrium vs. time and the displacements are recorded throughout the liquid. Whenever an atom has travelled a unit distance λ in a layer (which could represent, for example, the distance between two adsorption sites on the solid surface or the distance between two interfacial liquid layers for perpendicular, or inter-layer, movements, depending on what is the controlling step), the time for this displacement is inverted and a frequency is associated with this particular jump. It has to be noted that the advancement of the contact line is the result of collective atomic behavior; therefore λ is more an effective parameter that represents the

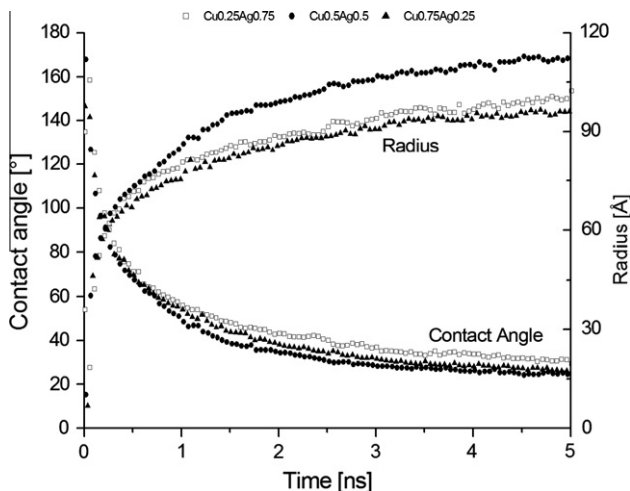


Fig. 1. Drop radius with the corresponding contact angle, determined by a circular interpolation, vs. time.

Table 1

Fitting parameters (γ/ζ_0 , equilibrium contact angle θ_0) for the three different alloy concentrations considered ($X_{Cu} = 0.25, 0.5$ and 0.75).

Liquid	γ/ζ_0 (m s^{-1}) (error)	θ_0 ($^\circ$) (error)
$\text{Cu}_{0.25}\text{Ag}_{0.75}$	2.02 (1.79)	13.53 (0.11)
$\text{Cu}_{0.5}\text{Ag}_{0.5}$	7.71 (1.33)	31.91 (0.55)
$\text{Cu}_{0.75}\text{Ag}_{0.25}$	3.64 (1.59)	12.05 (0.18)

A coupled parameter γ/ζ_0 is used in the fitting to make no assumptions on the surface tension.

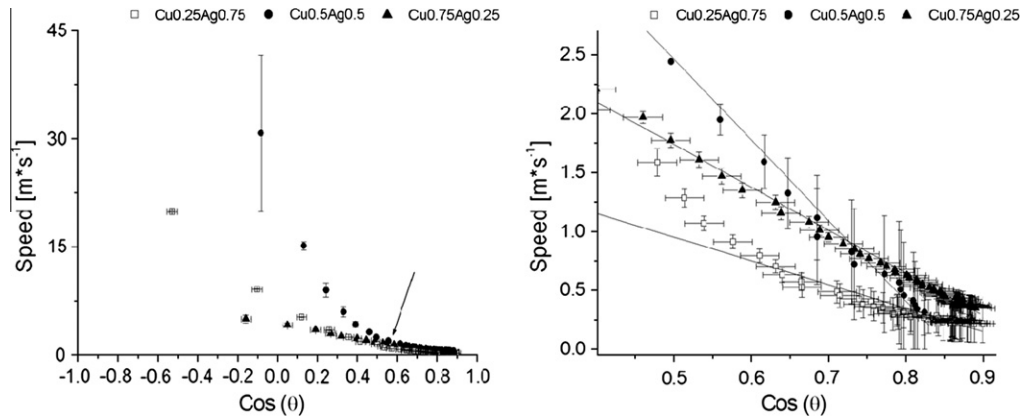


Fig. 2. The dynamic data is presented with the fitted curves that are made when the regime becomes stationary, toward equilibrium (for $\text{Cu}_{0.25}$ it started after the angle was below 50° and close to 60° for Ag contents of 50 and 75%). These values are recovered in dissolutive wetting experiments [19]. The range was determined by a maximization of R^2 . The linear zone starts after the arrow on the left; the linear fits that were applied are shown at higher magnification on the right. Although one could agree that there might be visually different linear portions, the linear fit has meaning when the contact angle approaches the equilibrium one.

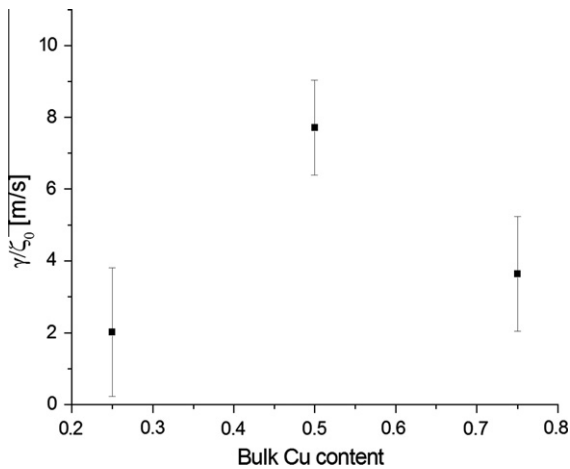


Fig. 3. The parameter γ/ζ_0 is displayed vs. the Cu content at the interface. A maximum occurs at around 50% Cu content.

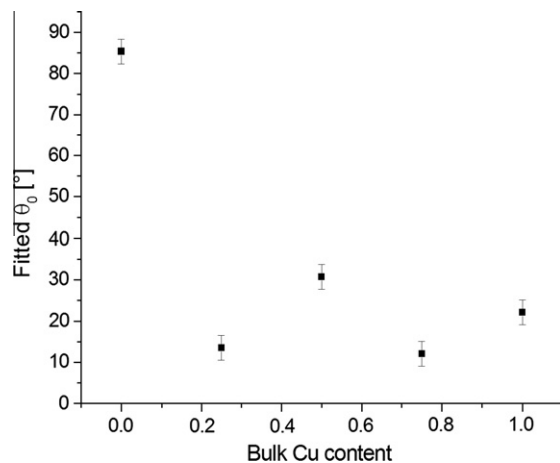


Fig. 4. Fitted equilibrium contact angle vs. the Cu content of the alloy. The contact angle is in the range 10 – 30° for the whole range of alloy concentration. The error on the contact angle was fixed to 3° . The pure Cu and Ag point are taken from Refs. [9,10]. The high contact angle for Ag was possibly caused by geometrical effects at the solid–liquid interface [10].

typical unit distance for atomic jumps. Our previous work shows that for liquid metals λ is typically of the order of interatomic distances (0.2–0.3 nm) [1,5,9,10,19].

As for other high-temperature systems, we observed here a strong ordering of the liquid atoms close to the solid–liquid interface [10,35]. The atomic frequencies in this ordered region are very different from those in the bulk region. A sampling is performed for the different possible jumps (from layer 1 to layer 2, layer 2 to 3, 3 to 2, etc., with layer 1 the closer to the solid surface) and each time an atom has left one layer and reaches the next it is accounted for in a distribution. These distributions are nearly normally distributed (because the solid substrate is impenetrable, there is a lack of symmetry in the problem), with an associated peak as the average and standard deviation as the error. Out of these distributions, it is assumed that the smallest calculated frequency will be rate-determining and characteristic of equilibrium. The authors have used this method in previous simulations [5] and proved that the movements from layer 3 to layer 2 were the determining ones for the dynamics in some liquid metals systems. We call this frequency k_{32} . Here, we followed all the atoms without making a distinction of their type (silver or copper) and accounted for all the atoms that travelled between the different layers.

From these frequency values, it is straightforward to estimate the surface tension from the linear fitting parameter γ/ζ_0 by imposing a spacing of 0.3 nm which is characteristic of Cu–Cu, Ag–Ag and Ag–Cu first-neighbor distances [9,10]. We expect the first few layers to adopt an fcc structure, and atoms in this structure can be separated by the lattice distance of Ag or Cu (4.09 and 3.65 Å respectively) for the second nearest neighbors and $\sqrt{2}/2 \times$ lattice distance.

The estimated γ are included in Table 2. Note that they underestimate the reported γ for simulations of Cu–Ag but are well within the physical meaning (reported EAM values

Table 2

Comparison between the two ways to estimate the interfacial surface tension γ : calculated directly using the liquid slab method and estimated from the fitted parameter γ/ζ_0 .

	Calculated γ (N m ⁻¹)	Fitted γ (N m ⁻¹) with $\lambda = 0.3$ nm	Fitted γ (N m ⁻¹) with $\lambda = 0.1$ nm
Cu _{0.25} Ag _{0.75}	0.265 (0.048)	0.121 (0.055)	0.326 (0.041)
Cu _{0.5} Ag _{0.5}	0.353 (0.068)	0.295 (0.144)	0.797 (0.119)
Cu _{0.75} Ag _{0.25}	0.457 (0.04)	0.303 (0.121)	0.818 (0.088)

ζ_0 is calculated by varying the parameter λ between 0.1 and 0.3 nm, a distance characteristic of the equilibrium distance between two metal atoms.

are 0.6–0.8 N m⁻¹) [30] and simulations are known for underestimating the surface tension of metals, which are measured to be, at 1150° C, 1.36 N m⁻¹ for pure Cu [5] and 0.886 N m⁻¹ for Ag [5]. With LAMMPS, a new series of calculations were performed to measure γ in the simulation by isolating slabs of the alloys in an Number of particles, Volume and Temperature (NVT)-equilibrated system by evaluation of the components of the pressure tensor. The statistics were evaluated in an Number of particles, Volume and Energy (NVE) system to prevent the thermostat from altering the atomic trajectories. Periodic boundary conditions were employed in the xy direction and the system size was comparable to the drop systems (simulated drops were 32,000 in size and slabs of 20,000 atoms were constructed) to obtain consistent values.

As can be seen, the agreement is good, at least insofar as the trend is recovered as the surface tension increases linearly with increasing Cu content. While these values remain underestimates of experimental surface tension values [5], the agreement reinforces the fact that the values calculated independently from the direct calculations and from the fit are consistent.

The direct comparison of K_0 and γ from the calculation and the fits is presented in Fig. 5. The fitted parameters and the calculated values overlap, demonstrating that the linear

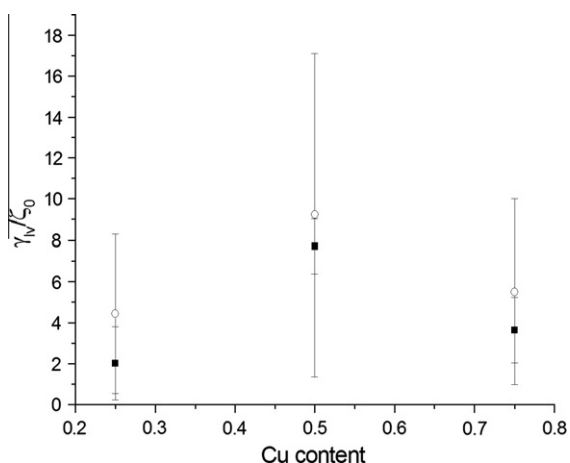


Fig. 5. Comparison between the fitted parameter and its direct calculation in the simulation. The open circles represent the measured parameters while the squares are the fitted values. The calculated ζ_0 is obtained by fixing λ at 0.3 nm, consistent with the interpretation of the model and previous work by the authors. The error bars are a combination of the errors in the calculations of γ and K_0 .

MKT model effectively describes the dynamics of spreading in the vicinity of equilibrium for these simulations. As a consequence, the dynamic evolution of the contact angle will only be dictated by equilibrium variables (ζ_0 and θ_0). The fitted parameter γ/ζ_0 is compared to a “calculated estimated parameter” $(\gamma/\zeta_0)_{\text{calc}}$ with the calculated friction ζ_0 .

3.4. Demixing in the Ag–Cu drops

The validation of the MKT is non-trivial in the case of alloys. The use of a coupled parameter γ/ζ_0 was designed to avoid imposing the surface tensions as the content can vary from the surface to the bulk.

All the different alloy compositions showed the same trend: copper enrichment at the solid–liquid interface, silver segregation at the surface of the liquid drop and formation of a silver monolayer ahead of the triple line on the solid surface. The existence of adsorbed layers on the solid surface was also observed for pure Ag liquids in other simulations by the authors [5], as well as in previous studies by Moon et al. [31] and Hashibon et al. [32,33], these layers growing by surface diffusion. In all cases, the atomic concentration of this layer was close to 1 in Ag.

Another way to characterize the liquid composition at the interfacial region is to evaluate the degree of Cu enrichment (the extent of this region was determined to be 20 Å from density calculations) vs. the bulk content of the alloy vs. time (actually, the liquid is richer in Cu at the core of the drop, and more Ag is present at the periphery and in the adsorbed layer on the solid surface). An example of the change in concentration across the solid/liquid interface is shown in Fig. 7, where the concentration in the liquid column and the drop is compared. The periodic boundary conditions designed in the liquid column configuration precludes adsorption on the solid–vapor interface (because of the absence of a free boundary in xy) and results in a more homogeneous and equilibrated liquid for the calculation of jump frequencies. In the drop, the Cu content close to the solid can increase by up to 60% in the Cu₂₅Ag₇₅ alloy and the Cu distribution equilibrates faster in the liquid reservoir configuration. In the liquids richer in copper, the Cu distribution is more stable as the degree of copper migration is limited (at 75% Cu content the difference between the bulk and the solid–liquid interface does not vary more than 5%).

Not only does silver separate at the triple junction and give rise to a monolayer film ahead of the liquid front on

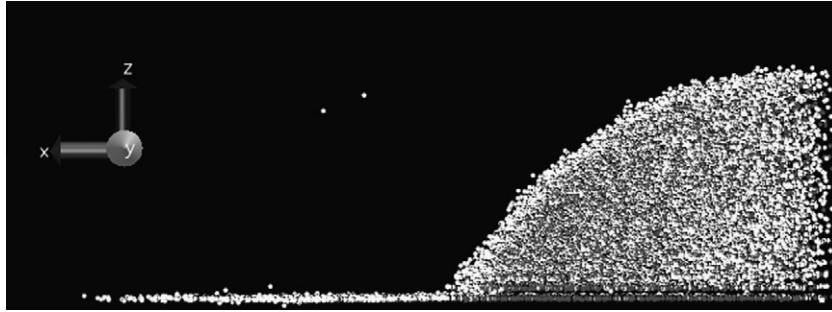


Fig. 6. Snapshot showing demixing in the drop. The Ag atoms (in white) are more concentrated at the external surface and in the first adsorbed layer at the very last frame of the simulations – at 5000 ps here in the case of the $\text{Cu}_{0.75}\text{Ag}_{0.25}$ alloy. The first layer was the first one affected by demixing as the second and upper layers have the same content as the bulk; therefore size effects are irrelevant. Copper atoms are represented by dark grey atoms.

the solid surface, but concentration measurements in the different shells of the droplet revealed that Ag segregates at the liquid–vapor interface. This again points to the fact that, due to its lower surface tension, liquid silver is more likely to segregate at the drop surface (Fig. 6). Yu and Stroud [34] have shown in MD simulations how a component with a lower surface tension will tend to migrate towards the surface.

In the plane, for the first layer in contact with the solid surface, the atomic structure change as shown by the correlation function $g(r)$ (in Fig. 8) is noticeable. It seems that, except for pure silver, the disposition of the atoms at the interface mimics the Cu solid structure with atoms separated by the average Cu–Cu distance. Adding Cu to an Ag drop will modify the interface, which will become mostly Cu by migration. This arrangement at the base of the drop thus seems logical. Ahead of the triple line Ag is adsorbed on the solid surface, extending in a monolayer. The presence of an adsorbed layer in front of partially wetted Cu drops on Ta was first shown in simulations by Hashibon et al. [32,33]. The thermodynamic stability of this layer has been proven with Density Functional Theory (DFT) calculations [32]. Benhassine et al. [9,10] also obtained similar behavior for pure Cu, Ag and Au on fixed surfaces.

As seen in previous simulations [9], Cu tends to freeze in contact with a fixed Ni substrate, which could indicate that

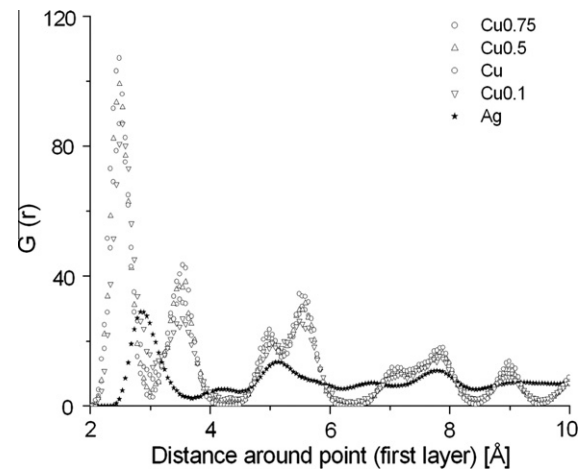


Fig. 8. Pair correlation functions for different compositions in the first layer in contact with the solid surface. The figure represents the mapping of atoms in this layer, showing that adding Cu to pure Ag creates a liquid structure closer to pure Cu in contact with the solid, meaning that any Cu in the liquid will be more dense at the contact point with the solid with which it has better affinity. Pure Ag and Cu pair-correlation functions were added to the plots for direct comparison.

the formation of the adsorbed layer of pure Ag surface ahead of the triple junction is more a kinetic effect: silver diffusion is faster. A possible microscopic interpretation could be that Ag atoms are more mobile in contact with

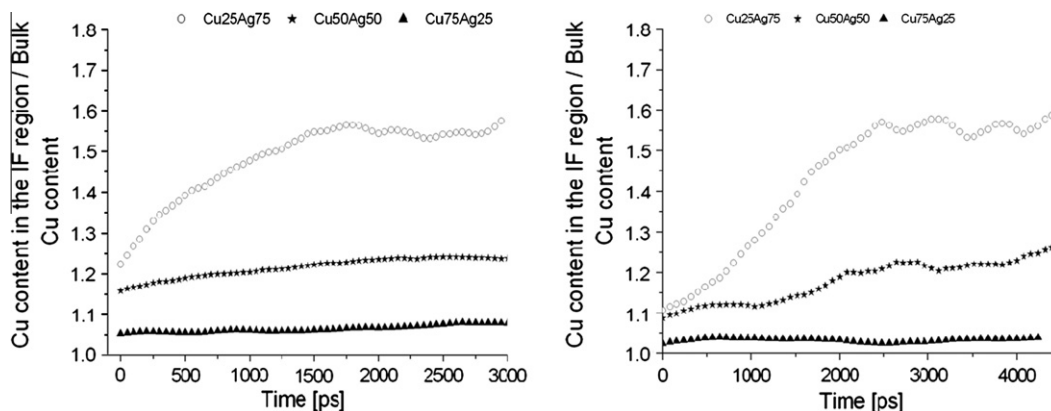


Fig. 7. Cu enrichment in the interfacial region with the solid vs. time for the liquid reservoir (left) and drop (on right).

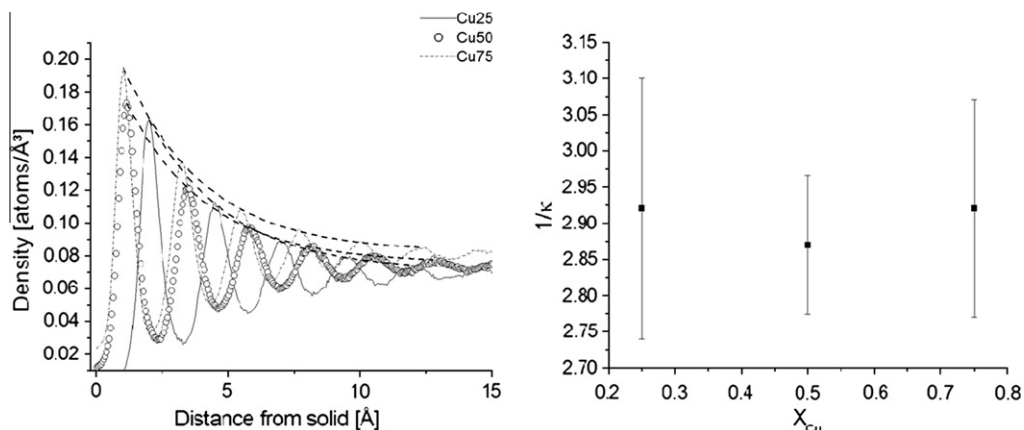


Fig. 9. Density profiles of the different alloys ($Cu_{0.25}$, $Cu_{0.50}$ and $Cu_{0.75}$). The decaying parameter of a fitting permits the liquid ordering vs. atomic content to be characterized. The density profiles take all the atoms into account without any distinction of type (Cu or Ag).

the surface due to the mismatch between silver and nickel; they can more easily diffuse away than copper, which is more strongly attracted by the solid surface and is more commensurate with the surface adsorption sites [9].

As previously shown [9], the density profiles can characterize the ordering at the interface and highlight a number of differences between the $Cu_{0.25}$, $Cu_{0.50}$ and $Cu_{0.75}$ alloys. It is well accepted that liquid metal interfaces present a strong ordering [9,10,31,35,36]. The overall densities of Cu and Ag as functions of the distance to the solid–liquid interface were fitted by a decreasing exponential to characterize the liquid metal ordering, as originally proposed by Hashibon et al. [35,36]. The decaying parameter $1/\kappa$ was plotted vs. copper content (Fig. 9). At an even Cu–Ag content, a small value of $1/\kappa$ was obtained that corresponds to a maximum in γ/ζ_0 (Fig. 5). This could indicate that the liquid is less organized at 50% than for contents of 25% and 75% copper, and agrees with previous results that show how, in liquid metal systems, a decrease in interfacial ordering may trigger a decrease in triple-line friction [10]. Although the error bars are significant and caution must be used in interpreting the results, it seems that the trend is recovered, i.e. the ordering seems to reach a minimum at 50% Cu atomic content.

4. Concluding remarks

The wetting of binary Cu–Ag alloys was simulated with molecular dynamics. The dynamic behavior of the wetting process is described well by the linear MKT model with a coupled parameter γ/ζ_0 , in agreement with other simulations and experiments of metal/metal wetting at high temperature in a nonreactive regime. The fitted parameters of the model were calculated from atomic trajectories and agreement was obtained. An optimum in γ/ζ_0 was observed at 50% Cu atomic content, and this trend was recovered in the direct calculations. The use of a coupled parameter was justified because of a dynamic rearrangement of the atomic content close to the solid, as revealed by the concentration

profiles. The ordering of the liquid was characterized by an exponential fitting that indicates slightly less organized interfaces that could account for a better mobility of the atoms in the liquid in the frame of the MKT.

These results support the idea that the microscopic features of the liquid–solid interface play a dominant role on the macroscopic contact angle and drop advancement, as was demonstrated for a wide range of metallic liquids in the nonreactive regime.

Acknowledgements

M.B. is grateful to the F.N.R.S of Belgium under the fonds pour la Formation à la Recherche dans l'Industrie et dans l'Agriculture. This work was also supported by the Director, Office of Science, Office of Basic Energy Sciences, Division of Materials Sciences and Engineering, of the US Department of Energy under Contract No. DE-AC02-05CH11231.

References

- [1] Saiz E, Tomsia AP. *Nat Mater* 2004;3:903–9.
- [2] Asthana R, Sobczak N. *JOM-e* 2000; 52(1). <<http://www.tms.org/pubs/journals/JOM/0001/Asthana/Asthana-0001.html>>.
- [3] Yost FG, Sackinger PA, O'Toole EJ. *Acta Mater* 1998;46:2329.
- [4] Warren JA, Boettinger WJ, Roosen AR. *Acta Mater* 1998;46:3247.
- [5] Saiz E, Tomsia AP, Rauch N, Scheu C, Rühle M, Benhassine M, et al. *Phys Rev E* 2007;76:041602.
- [6] Kozlova O, Voytovych R, Protsenko P. *J Mater Sci* 2010;45(8):2099–105.
- [7] Grigorenko N, Poluyanskaya V, Eustathopoulos N, Naidich Y. In: Bellosi A, Kosmac T, Tomsia AP, editors. *NATO advanced science institute series. Sub-series 3. Interfacial science in ceramic joining*, vol. 58. New York: Springer; 1998. p. 57–67.
- [8] Yin L, Murray BT, Su S, Sun Y, Efraim Y, Taitelbaum H, et al. *J Phys Condens Matter* 2009;21(46):464130.
- [9] Benhassine M, Saiz E, Tomsia AP, De Coninck J. *Langmuir* 2009;25(19):11450–8.
- [10] Benhassine M, Saiz E, Tomsia AP, De Coninck J. *Acta Mater* 2010;58:2068–78.
- [11] Blake TD, Haynes JM. *J Colloid Interface Sci* 1969;29:174.

- [12] Blake TD. PhD Thesis, University of Bristol; 1968.
- [13] Rauch N, Saiz E, Tomsia AP. *Z Metallkd* 2003;94(3):233.
- [14] Webb III EB, Grest GS, Heine DR, Hoyt JJ. *Acta Mater* 2005;53:3163.
- [15] Landry K, Eustathopoulos N. *Acta Mater* 1996;44:3923.
- [16] Mortensen A, Drevet B, Eustathopoulos N. *Scripta Mater* 1997;36:645.
- [17] Saiz E, Tomsia AP, Cannon RW. *Acta Mater* 1998;6:2349.
- [18] Eustathopoulos N. *Acta Mater* 1998;46:2319.
- [19] Saiz E, Benhassine M, De Coninck J, Tomsia AP. *Scripta Mater* 2010;62(12):934–8.
- [20] de Ruijter MJ, Blake TD, De Coninck J. *Langmuir* 1999;15:7836.
- [21] Plimpton SJ. *J Comput Phys* 1995;117:1–19.
- [22] Stevens M, Plimpton SJ, Pollock R. In: Proceedings of the eighth SIAM conference on parallel processing for scientific computing, Minneapolis, MN; 1997.
- [23] Daw MS, Baskes MI. *Phys Rev B* 1984;29(12):6443–53.
- [24] Foiles SM, Baskes MI, Daw MS. *Phys Rev B* 1986;33:7983–91.
- [25] Bertrand E, Blake TD, Ledauphin V, Ogonowski G, De Coninck J, Fornasiero D, et al. *Langmuir* 2007;23:3774.
- [26] Blake TD, Clarke A, De Coninck J, de Ruijter MJ. *Langmuir* 1997;13:2164.
- [27] Adaõ MH, de Ruijter MJ, Voué M, De Coninck J. *Phys Rev E* 1999;59:746.
- [28] Efron B, Gong G. *Am Statistician* 1983;37:36.
- [29] Seveno D, Vaillant A, Rioboo R, Adaõ H, Conti J, De Coninck J. *Langmuir* 2009;25(22):13034–44.
- [30] Webb III EB, Grest GS. *Phys Rev Lett* 2001;86(10):2066.
- [31] Moon J, Yoon J, Wynblatt P, Garoff S, Sutter RM. *Comput Mater Sci* 2002;25:503–9.
- [32] Hashibon A, Elsässer C, Mishin Y, Gumbsch P. *Phys Rev B* 2007;76:245434.
- [33] Hashibon A, Lozovoï AY, Mishin Y, Elsässer C, Gumbsch P. *Phys Rev B* 2008;77:094131.
- [34] Yu W, Stroud D. *Phys Rev B* 1997;56(19):12243–9.
- [35] Hashibon A, Adler J, Finnis MW, Kaplan WD. *Interface Sci* 2001;9:175–81.
- [36] Hashibon A, Adler J, Finnis MW, Kaplan WD. *Comput Mater Sci* 2002;24:443–52.